Measurements and Simulations of Weld Residual Stresses for Feeder Dissimilar Metal Welds

Y. Shi[1], X. Duan[1♣], M. Wang[1], M. Li[2]

[1]Compoent Integrity, Candu Energy Inc.

2285 Speakman Drive, Mississauga, Ontario, Canada L5K 1B1

[2]Major Components Engineering Department, Ontario Power Generation Inc.

889 Brock Road, Pickering, ON L1W 3J2

Abstract

In CANDU nuclear power plants, dissimilar metal welds (DMWs) are present in some of the feeders. PWR operating experience and research suggest that such dissimilar metal welds on outlet feeders may be susceptible to primary water stress corrosion cracking (PWSCC) especially at the welding start/stop locations. In this paper, a finite element method (FEM) approach has been developed through an ABAQUS user subroutine to predict welding residual stress (WRS) in DMWs. Measurement results from the X-ray diffraction and the contour methods are adopted to validate the WRS prediction. Sensitivity studies on the effect of work hardening and annealing on WRS prediction are also investigated. The predicted WRS will be applied as inputs to the natural crack growth analysis to demonstrate the crack stability in the near future.

1. Introduction

Operating experience from pressurized water reactors (PWRs) piping butt welds suggests that DMWs may be susceptible to PWSCC especially at the high residual stress locations associated with welding repair and the welding start/stop location. In CANDU nuclear power plants, DMWs are present in some of the outlet feeders, of which DMWs are buttwelded with carbon steel and Inconel 600. Candu Energy has been contracted by Canadian utilities to establish a Leak-Before-Break (LBB) case to support the continued safe operation of feeder DMW. Candu Energy has funded a product development project in 2014 to develop the capability of simulating the welding process to predict the WRS, and to assist the development of novel welding procedures. In the process, the stringent quality assurance requirements (CSA Z299.1, the applicable elements in CSA N286-05 and Sections 5 to 11 inclusive of CSA N286.7) related to the pressure boundary assessment of Class 1 component are met.

In the present work, a heat source model, based upon the computational welding mechanics in references [1-2], is adopted and implemented into a commercial finite element code ABAQUS through user subroutines. To provide a direct and systematic validation of the WRS model, dissimilar metal welding samplers are firstly fabricated, and then the X-ray diffraction and the contour methods are employed to measure the WRS in the weld and the heat affected zones (HAZ). Three phases of modeling activities are followed:

- Phase 1: pre-fabrication modeling of the welding process. The results are used to select the locations for temperature and strain measurements.

♣ Corresponding author. Email address: Xinjian.Duan@snclavalin.com. Tel.: +1 905 823 9040 x 36646.

- Phase 2: calibration of the FEM thermal modeling parameters (related to the thermal model) to match the recorded temperature profiles for one weld, and then compare the predicted temperature profiles for other welds, which are fabricated with different welding parameters. This phase is completed before the WRS measurements.

- Phase 3: calibration of the FEM material modeling parameters to match the measured WRS stress field with those measurements from the X-ray diffraction and contour methods. Sensitivity studies are also employed to further understand the impact of some modeling parameters on the predicted WRS. The bounding WRS profiles are then determined for the future natural crack growth modeling to demonstrate the safety margins against pipe rupture.

The focus of the present paper is Phases 2&3 modeling and measurement activities.

2. WRS Measurements

2.1 Sample fabrications

The dissimilar metal welding samplers are fabricated with Inconel Alloy 600 and SA-106 Grade B carbon steel by automatic welding apparatus as shown in Figure 1(a). Each sample is manufactured from two pieces of NPS 2½ SA-106 Gr. B pipe of 6 inches long on either side of one NPS 2½ Inconel Alloy 600 pipe of 8 inches long. Both materials are procured to nuclear grade with all mandatory documents. Type K thermocouples are used for the temperature measurement at various locations near the welding pool. The recorded temperature histories are used to calibrate the thermal and welding parameters used in the welding heat transfer models. Vishay strain gauges were also amounted to check the thermal strain. There are four welding passes: three normal passes with weldment deposit and a final wash pass, of which no material deposits. The welding parameters are chosen according to the welding specifications, some variations on the welding current, voltage and welding speed have been made for the purpose of sensitivity study. All fabricated samples are thoroughly examined by visual inspection, liquid penetration examination and radiographic examinations to meet the requirements in Article 9 of Section V of ASME BPVC.

2.2 X-ray residual stress measurement

The welding residual stresses of fabricated samples are measured by two residual stress measurement techniques: the X-ray diffraction and the contour method. A brief introduction of experimental techniques and procedures are outlined, while the measured results in comparison to modeling predictions will be discussed in Section 4.

The X-ray diffraction technique uses the distance between crystallographic planes, i.e., *d*-spacing, as a strain gauge. When the material is in tension, the *d*-spacing increases and when the material is under compression the *d*-spacing decreases. This method can only be applied to crystalline, polycrystalline and semi-crystalline materials. The presence of residual stresses in the material produces a shift in the X-ray diffraction peak angular position which is directly measured by the detector. In this exercise, the WRS measurement is performed using a 2.0 mm round aperture for near O.D. locations and a 1.0 mm x 2.0 mm aperture for near I.D. locations at three zones in axial direction, specified as weld centerline, Alloy 600 HAZ and carbon steel HAZ. Circumferentially, the sampling points are placed near the welding stop location, where the high likelihood of the highest tensile stress is present. Both hoop and axial stresses are measured. However, only the axial stress results are reported due to the factor that axial stress is the driving force for the initiation and growth of circumferential crack, which is more limiting than axial crack (because axial crack has a limited length) from the structural integrity point of view. The X-ray experiment setup is shown in Figure 1(b).

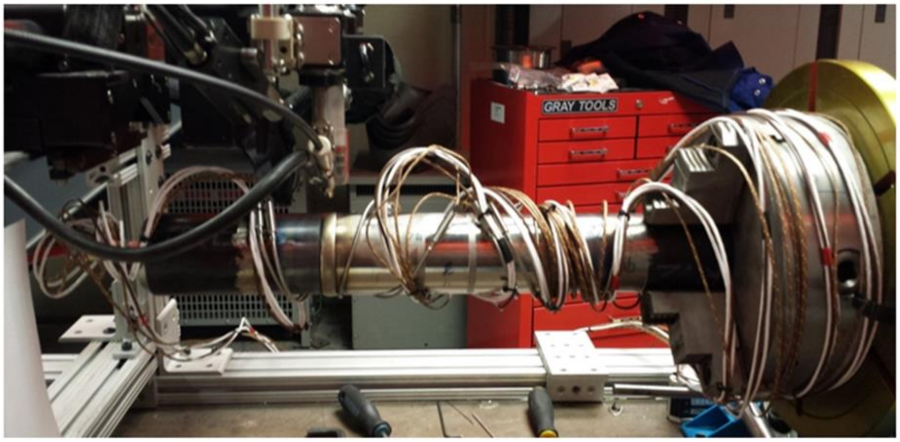

(a)

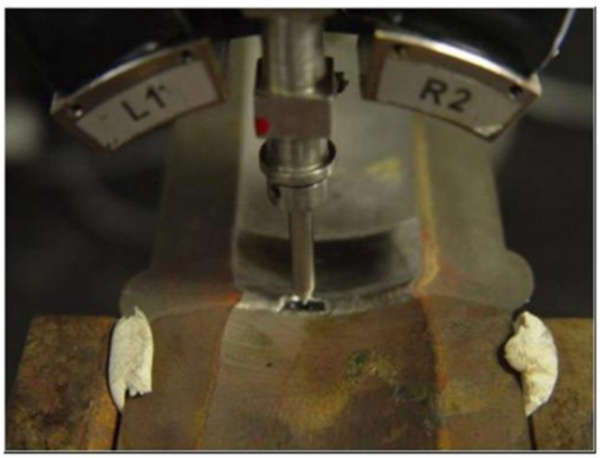

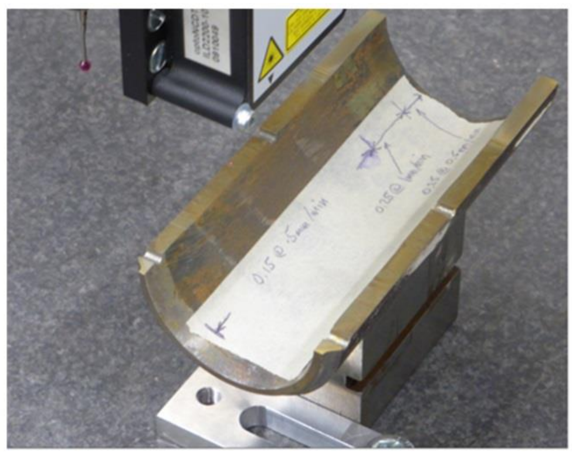

(b) (c)

Figure 1 Weld fabrication and WRS measurement, (a) welding setup with instrumentations, (b) the X-ray WRS measurement; (c) the contour WRS measurement.

2.3 The contour method residual stress measurement

The contour method is based on an elastic superposition principle. Experimentally, the sample is cut in two and the parts will deform from the release of the internal stresses. After measuring the contour (or shape) of the newly created surface of deformed shape, the method analytically forces the cut surface back flat and calculate the original residual stresses normal to the cut plane. The contour method provides a full 2D stress map over the plane of interest and the measured stresses are not sensitive to microstructural variation. In the present work, both the axial plane and the circumferential plane have been investigated, which generated both hoop stress and axial stress maps. Figure 1(c) presents the deformed surface measurement of the axial plane. For the axial stress measurement, attention is focused on the Alloy 600 HAZ region as the highest axial tensile stress is likely located. Both the X-ray and the contour measured results will be reported and compared with prediction in Section 4.

3. Weld Residual Stress Modeling

Moving heat source [1] defines the heat flux on the surface of the weld as a power density function throughout the volume of the weld. For arc welds, an ellipsoid with a Gaussian distribution of flux on the surface of the weld defines the temperature profile in the welding pool. The power distribution function is defined by the equation:

$$q(x,y,z,t) = \frac{6\sqrt{3}fQ}{abc\pi\sqrt{\pi}} e^{-3x^2/a^2} e^{-3y^2/b^2} e^{-3[z+v(\tau-t)]^2/c^2} \quad (1)$$

where, v is the welding speed; t is the welding time; f is the power fraction; Q is the heat energy input; x, y and z are the Cartesian coordinates centred on the surface of the specimen at the torch start position; τ is a lag factor to define the position of the source at time t=0. The heat input for the moving heat source is represented by an ellipsoidal distribution defined by the non-dimensional effective torch radius, which is the distance from the torch centre to the locations in the specimen. The welding pool shapes is defined by the pool geometric parameter a, b, c. To simulate the feeder girth butt welding, the Cartesian coordinates need to convert to a cylindrical coordinate system.

The heat energy input Q is defined by the welding parameters as:

$$Q(x,y,z) = \eta VI \quad (2)$$

where, η is the heat source efficiency, V is the welding voltage and I is the welding current.

The heat loss due to the convection is taken into account through a convection boundary condition [2]. This boundary flux q_c in w/m^2 is applied on all external surfaces and computed from the following equations:

$$q_c = h_c(T - T_0) \quad (3)$$

$$h_c = 5 + 0.05(T - 300) + 6 \times 10^{-7}(T - 300)^3 \quad (4)$$

where h_c is the convection heat transfer coefficient defined as a function of the surface temperature and T_0 is the ambient temperature in kelvin (300 K).

The moving heat source Equations (1) and (2), along with the heat energy input Equation (4), have been implemented into ABAQUS/Implicit code through a user-defined DFLUX subroutine [3]. This subroutine provides the sole thermal load for the thermal calculation.

A 3D finite element model is set up and shown in Figure 2. A sequential thermal-stress coupled analysis is adopted, of which the temperature field is predicted by thermal analysis with the user subroutines described above, while the stress model predicts the stress field based upon the temperature history predicted by thermal model. A temperature dependent material model is used in the stress analysis. It is assumed that annealing occurs at specific temperatures for both carbon steel and Alloy 600. The hardening behavior of the material is also assessed and will be discussed in next section. For both thermal and stress analyses, the bead is deposited incrementally while the whole welding pool is treated as a dynamic welding pool domain with updated configuration at each time increment.

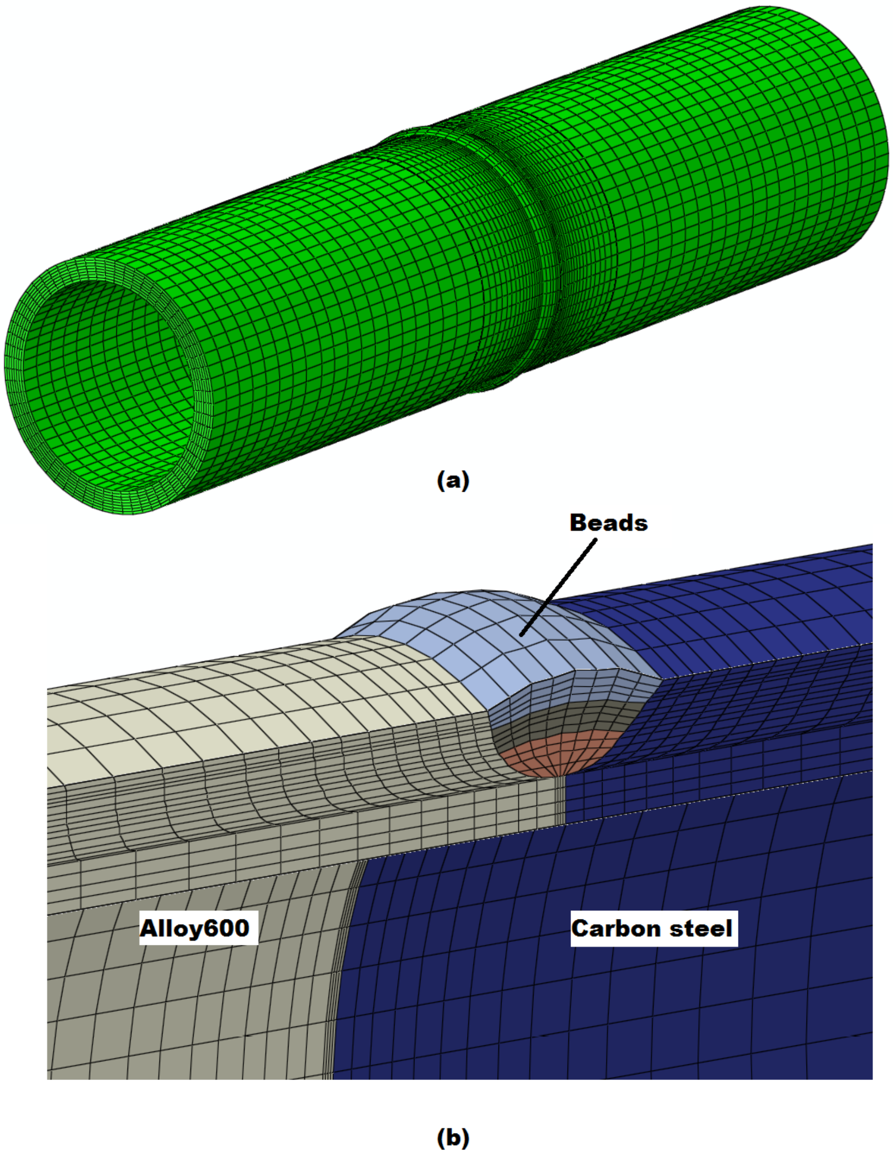

Figure 2 FEA Model setup, (a) mesh configuration; (b) enlarged view of dissimilar metal welding pool.

4. Results and Discussions

4.1 Temperature calibration in Phase 2

In the present work, the temperature calibration was made through adjusting the welding parameters to match the recorded temperature history at a specific location where the thermocouple is mounted. Figure 3 (a) shows the measured temperature history in comparison to the calibrated temperature at the point 5 mm from the weld center on the carbon steel side. Overall, the calibrated temperature matches well with the measured temperature history. It is worth mentioning that the temperature history is sensitive not only to the welding pool parameters (Eq. 1) and the energy input (Eq. 2), but also to the convection coefficient (Eq. 3) as well. The temperature field prediction based on the calibrated welding parameters is plotted in Figure 3 (b).

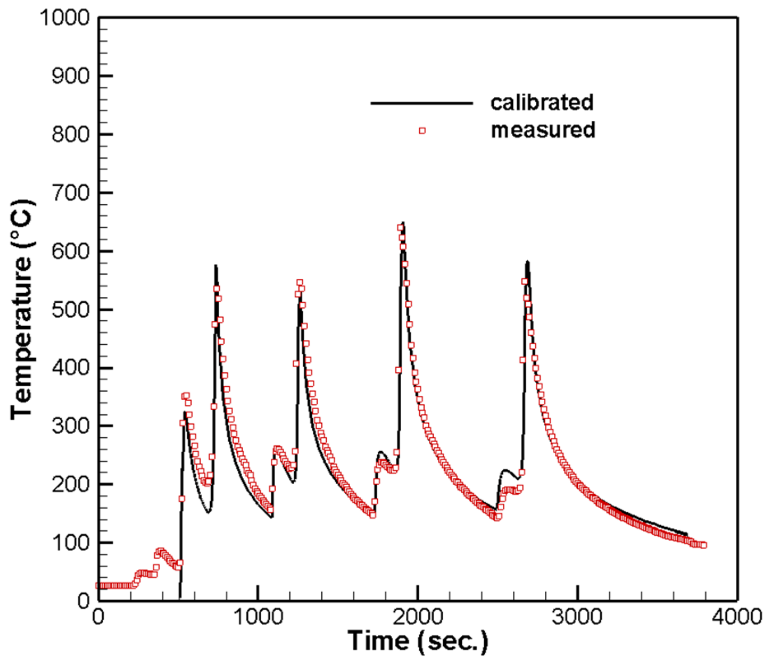

(a)

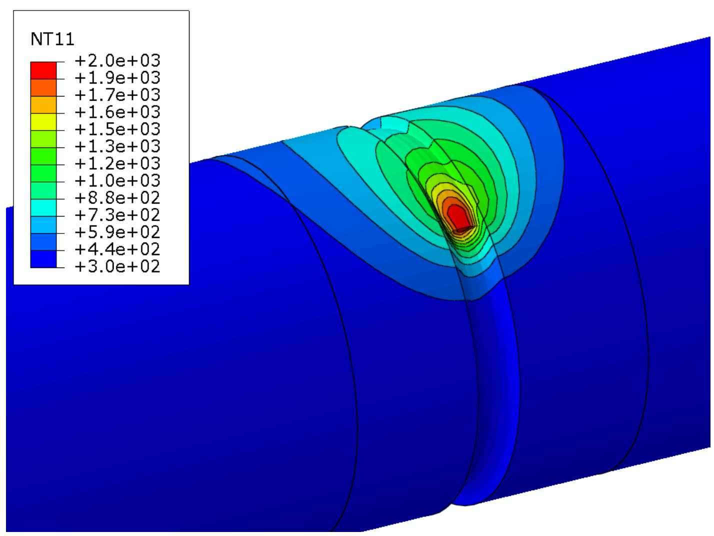

(b)

Figure 3 Temperature calibration, (a) temperature history calibrated at Alloy 600 side, 5 mm away from the weld center; (b) predicted temperature field after calibration (unit: K).

4.2 Blind validation

Blind validation was performed. The WRS distribution and magnitude are predicted prior to the X-ray and the contour stress measurement. The comparison of the measured X-ray WRS with predicted WRS is plotted in Figure 4. Two sections, which are more susceptible to cracking, are compared, one at HAZ near Alloy 600 side and the other at HAZ near carbon steel side. Reasonable agreements are obtained.

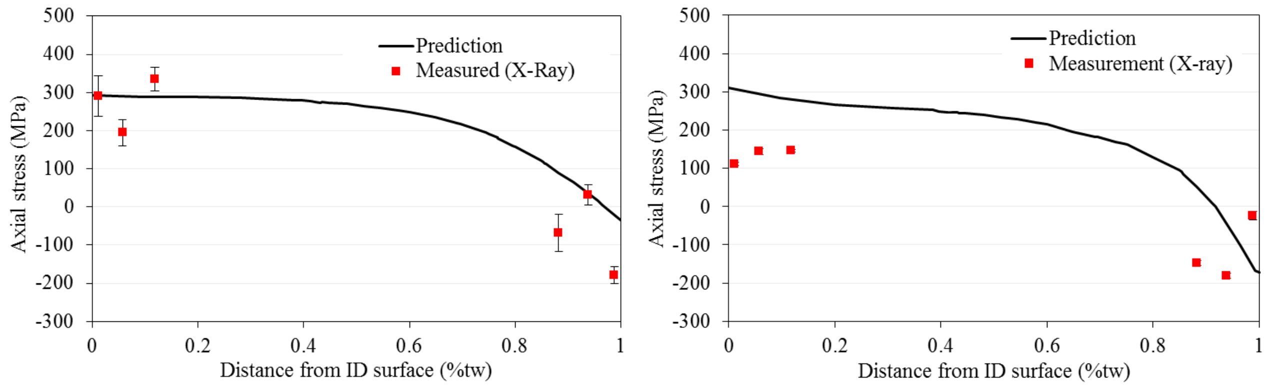

(a) (b)

Figure 4 Axial stress comparison, X-ray measurement vs prediction: (a) axial stress along the thickness at HAZ Alloy 600 side; (b) axial stress along the thickness at HAZ carbon steel side.

One of the planes of interest in the welded sample is a hoop plane at Alloy 600 side 2 mm from the weld center line, where the maximum axial stress is predicted by the FEM model. For the contour method, the hoop cutting plane is set accordingly. The measured axial stress in terms of stress map is plotted in Figure 5, while the predicted welding residual stresses are calculated in three ways: isotropic hardening, kinematic hardening and combined (averaged) stress of isotropic and kinematic hardening. The stress maps by measurement and prediction both show several interesting features:

1) the maximum stress locates at the stop location (30 degrees from 12 o'clock clockwise), and stop location is also the transition zone where the maximum tensile stress turns into the maximum compressive stress;
2) except for the transition zone, the OD surface shows compressive stress while the ID surface experiences tensile stress. This is also verified by the X-ray measurement; and
3) the FEM model predicts a very similar stress pattern as shown in the measured stress map.

In terms of stress magnitude, isotropic hardening model seems to slightly over-predict stress while kinematic hardening goes to the opposite. The combined model shows a very close stress magnitude against the measured stress. The materials in the welding pool and heat affected zone experience thermal cycles during welding, as illustrated in Figure 3 (a). The temperature cycling from heating cycle will cause the material experienced compression and tension periodically. Such cyclic deformation behavior could be best descripted by non-linear kinematic hardening material model. However, the tensile and compressive testing data are very difficult to obtain for material at more than 1000°C temperature. From an engineering perspective, USNRC [4] and EPRI [5] recommend that the combined (averaged) linear kinematic hardening and isotropic hardening would provide a better prediction. This approach has been confirmed by this modeling exercise as well.

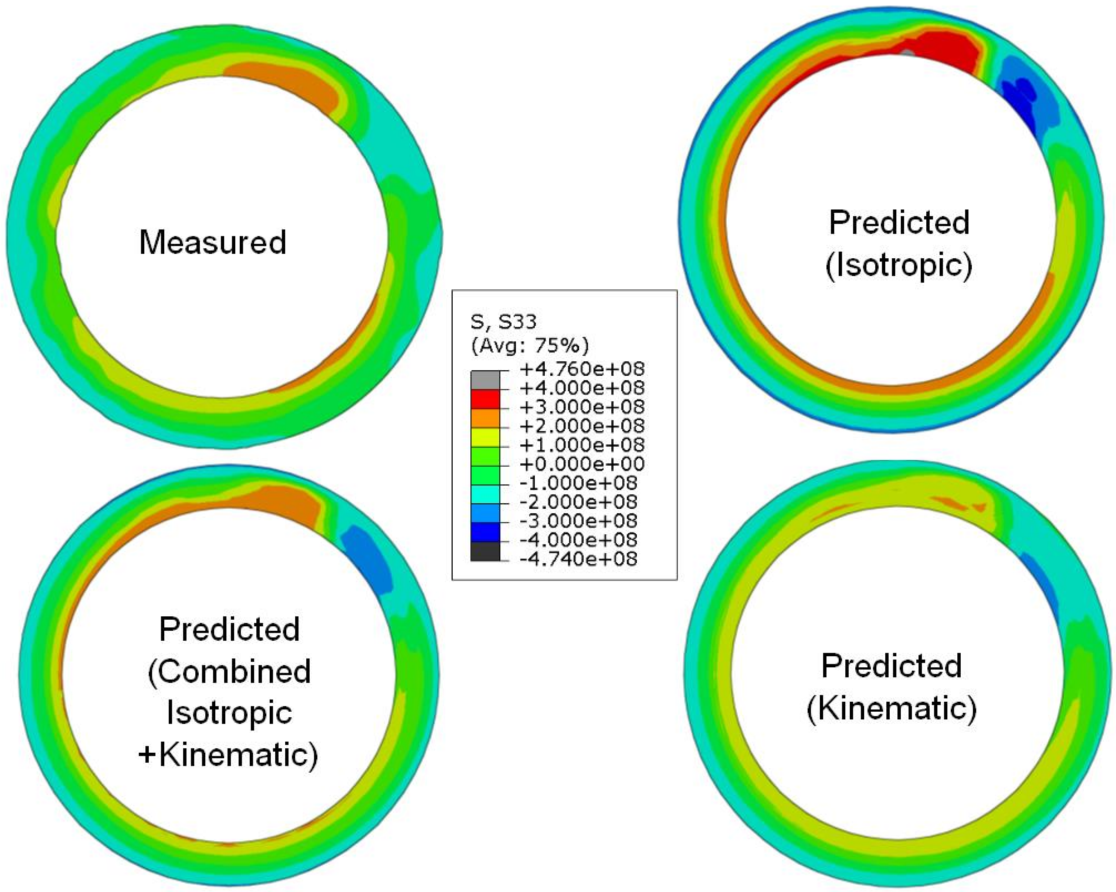

Figure 5 Comparison of axial stress in simulation and measurement.

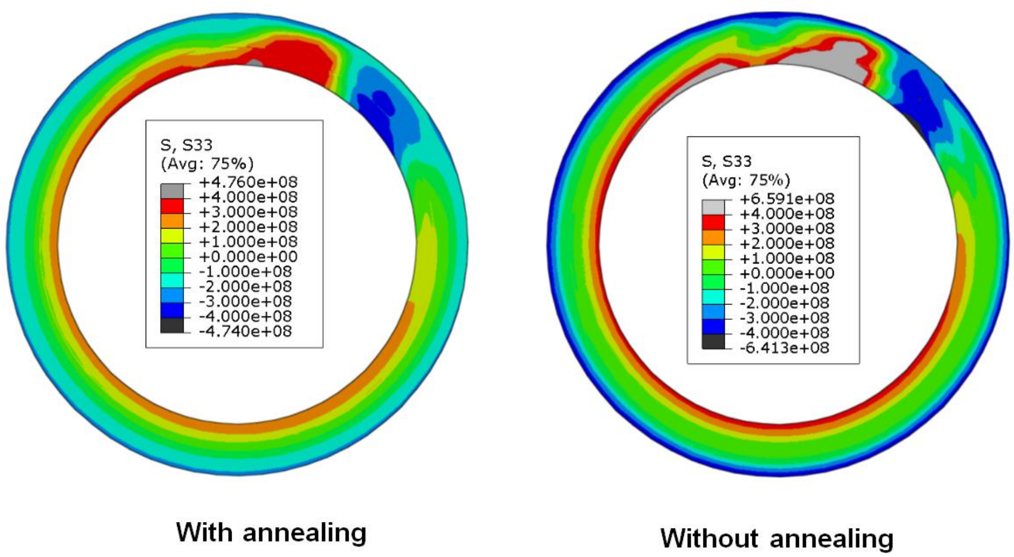

Figure 6 Effect of annealing on WRS prediction.

4.3 Effect of Annealing

Annealing refers to the metal recovery and recrystallization at high temperatures [6]. In the current model, a simplified annealing process is simulated through resetting the residual stress and state variables when the welding pool temperature at a specific location exceeds a target temperature. Figure 6 shows the effect of annealing on the WRS prediction. For the case without annealing, a high (more than 80%) WRS is predicted, which is far beyond the measured stress level.

5. CONCLUSION

A robust finite element WRS model has been developed and validated. The model validation show that this model is able to predict very similar stress pattern and stress magnitude in comparison to the stress measured by the contour method for feeder dissimilar metal weld. In terms of modeling techniques, annealing and combined isotropic and kinematic hardening are recommended.

This newly developed model is a generic tool and can be used not only for feeder DMWs but also for other welded components. The work is in full compliance with the required quality assurance program, CSA Z299.1, the applicable elements in CSA N286-05 and Sections 5 to 11 inclusive of CSA N286.7.

6. REFERENCE

[1] J. Goldak, A. Chakravarti, M. Bibby, *A New Finite Element Model for Welding Heat Source*, Metallurgical Transaction B, vol. 15B, 299-305, 1984.

[2] J. Goldak, *Distortion and Residual Stress in Welds: The next Generation*, Proceedings of the 8th International Conference on Trends in Welding Research, Pine Mountain, Georgia, USA, 2008 June 1-6.

[3] *ABAQUS User Manual*, version 6-13, 2013.

[4] USNRC, *Summary of Public Meeting and Webinar on the NRC/EPRI Weld Residual Stress Validation Program*, USNRC ADAMS File Number ML14352A195, 2014 December 18.

[5] EPRI Technical Report, 3002005499, *Materials Reliability Program: Welding Residual Stress Dissimilar Metal Butt-Weld Finite Element Modeling Handbook (MRP-317 Revision 1)*, Palo Alto, CA: 2015 September.

[6] I.S. Kim and J.S. Lee, *Effect of Intercritical Annealing Treatment on the Fracture Toughness of SA106 Gr. C Piping Steel*, Proceedings of 7th International Conference on Nuclear Engineering, Tokyo, Japan, 1999 April 19-23.